# Identification of Hydrogen Molecules in ZnO

E. V. Lavrov,* F. Herklotz, and J. Weber
*Technische Universität Dresden, 01062 Dresden, Germany*
(Received 16 March 2009; published 8 May 2009)

Hydrogen molecules in ZnO are identified by their local vibrational modes. In a Raman study, interstitial $H_2$, HD, and $D_2$ species were found to exhibit local vibrational modes at frequencies 4145, 3628, and 2985 $cm^{-1}$, respectively. After thermal treatment of vapor phase grown ZnO samples in hydrogen atmosphere, most hydrogen forms shallow donors at the bond-centered site ($H_{BC}$). Subsequently, $H_{BC}$ migrates through the crystal and forms electrically inactive $H_2$. These results imply that the ''hidden'' hydrogen in ZnO [G. A. Shi *et al.*, Appl. Phys. Lett. **85**, 5601 (2004)] occurs in the form of interstitial $H_2$.

DOI: 10.1103/PhysRevLett.102.185502 PACS numbers: 61.72.uj, 63.20.Pw, 78.30.Fs

Molecular hydrogen in semiconductors was predicted by theory to be stable more than 20 years ago [1,2]. Since then, properties of isolated interstitial $H_2$ were carefully studied in GaAs [3], Si [4–7], and Ge [8].

For ZnO, no direct experimental evidence for the presence of $H_2$ has been presented so far. Nonetheless, the $H_2$ molecule was assumed to be responsible for the so-called ''hidden'' hydrogen in ZnO, which is not seen by IR absorption but can be converted into a shallow donor in the course of sample processing [9]. For most ZnO applications, stable and reproducible *n* and *p* doping is a necessity [10,11]. Therefore, the uncontrolled influence of this hidden species on the electrical properties of ZnO is disastrous for applications and should be avoided.

Hydrogen is often present in the crystal growth environment, and it is very difficult to prevent its incorporation into the crystal during semiconductor processing. Device applications require a deep understanding of the behavior of hydrogen in ZnO; in particular, the nature of the hidden species has to be unraveled.

Interest in hydrogen in ZnO began in the 1950s, when Mollwo [12] and Thomas and Lander [13] showed that hydrogenation of ZnO at elevated temperatures gives rise to *n*-type conductivity. Since then, hydrogen in ZnO has been an object of active research [14–27]. First-principles calculations carried out by Van de Walle revealed that isolated hydrogen in ZnO acts as a shallow donor [28]. Recent experiments confirmed this theoretical prediction. Bond-centered hydrogen $H_{BC}$ primarily bound to the O atom with the O–H bond aligned parallel to the *c* axis was shown to be a shallow donor in ZnO with an activation energy of 53 meV [29]. It was established that bond-centered hydrogen is unstable against thermal treatment at 190 °C. The dominant sink for $H_{BC}$ was suggested to be the hydrogen molecule [29]. No direct experimental evidence, however, was presented in support of this model.

In this Letter we present the results of a Raman scattering study, which unambiguously shows the existence of $H_2$ in ZnO and supports the assumption that the hidden species in ZnO originates from hydrogen molecules.

The ZnO crystals used in this work were hexagonal prisms with a diameter of about 2 mm and a length of ~10 mm. The nominally undoped *n*-type single crystals with resistivity of 10–100 Ω cm were grown from the vapor phase at the Institute for Applied Physics, University of Erlangen (Germany) [30,31]. Hydrogen and/or deuterium was introduced via thermal treatment of the samples in sealed quartz ampoules, filled with $H_2$ and/or $D_2$ gas (pressure of 0.5 bar at room temperature). The treatments were performed at 1000 °C for 1 h and were terminated by quenching to room temperature in water. Under these conditions, the hydrogen concentration in ZnO directly after the treatment was around $10^{18}$ $cm^{-3}$ [12,13].

Raman measurements were carried out in a 90° geometry using the frequency doubled 532 nm line of a Nd:$YVO_4$ laser for excitation. The scattered light was analyzed using a single grating spectrometer and a cooled Si CCD detector array. Spectral resolution was 2.5–5 $cm^{-1}$. The measurements were performed with the sample mounted in a cold finger cryostat using liquid helium for cooling. During the measurements the temperature of the bulk sample was varied by an electrical heater. A detailed description of the Raman setup is given elsewhere [6].

The scattering geometry is defined with respect to the *c* axis of ZnO. The *x*, *y*, and *z* axes are parallel to the crystallographic orientations $[10\bar{1}0]$, $[1\bar{2}10]$, and *c*, respectively. In the notation $a(b, c)d$, $a(d)$ refers to the propagation vector of the incident (scattered) light, whereas $b(c)$ characterizes the polarization vector of the incident (scattered) light. The notation $a(b, -)d$ implies that the scattered light is measured without a polarizer.

Figure 1 shows Raman spectra recorded at $T \leq 20$ K from a ZnO sample treated in $H_2$ gas. A line at 3611 $cm^{-1}$ dominates the spectrum obtained directly after the treatment. This signal is due to a stretch local vibrational mode of a hydrogen-related defect originally labeled H-I [18]. Recent studies of hydrogen donors in ZnO revealed that H-I is an isolated hydrogen ($H_{BC}$) located at the bond-centered site of the ZnO lattice [29]. In as-hydrogenated samples, $H_{BC}$ is the dominant shallow donor with an

 

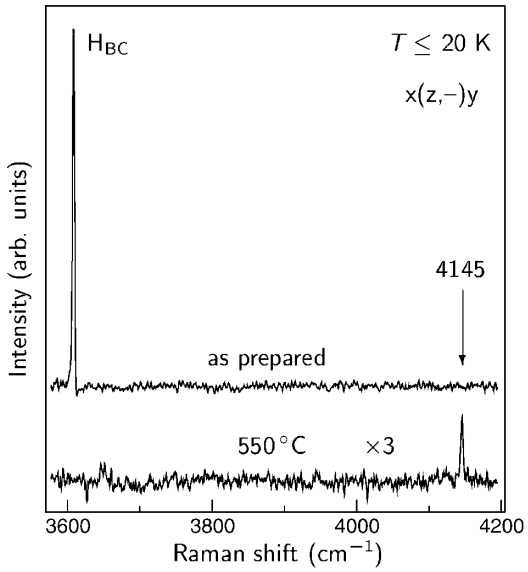


FIG. 1. Raman spectra of a ZnO sample measured at $T \leq 20$ K in the $x(z, -)y$ geometry. Top: Directly after hydrogenation; bottom: after subsequent anneal at 550 °C. Spectral resolution is 5 cm$^{-1}$. Spectra are vertically offset for clarity.

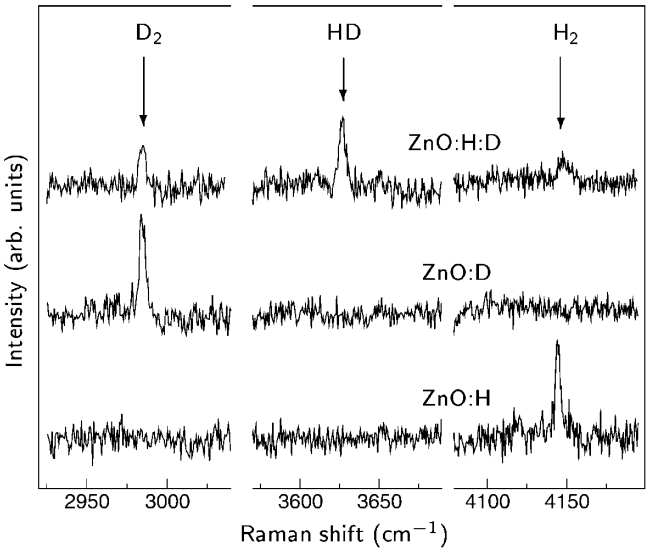


FIG. 2. Raman spectra of ZnO samples measured at $T \leq 20$ K in the $x(z, -)y$ geometry. The samples were treated at 1000 °C in $H_2$ (bottom), $D_2$ (middle), and $H_2 + D_2$ (top) gas and subsequently annealed at 550 °C. Spectral resolution is 5 cm$^{-1}$. Spectra are vertically offset for clarity.

ionization energy of 53 meV. For the samples of this study the donor concentration was around $10^{18}$ cm$^{-3}$.

Bond-centered hydrogen is known to be mobile already at room temperatures [29,32]. After annealing the ZnO sample at 550 °C for 30 min, the 3611 cm$^{-1}$ line disappears (see bottom spectrum in Fig. 1). A new line at 4145 cm$^{-1}$ shows up in the spectrum at the expense of the $H_{BC}$ signal. The frequency of this transition is close to that of free $H_2$ observed at 4161 cm$^{-1}$ [33].

The results of isotope substitution experiments are presented in Fig. 2, which shows Raman spectra obtained from ZnO samples treated in $H_2$ and/or $D_2$ gas. As follows from the figure, substitution of hydrogen by deuterium results in a redshift of the 4145 cm$^{-1}$ line to 2985 cm$^{-1}$. These modes plus an additional one at 3626 cm$^{-1}$ are detected in the sample treated in a mixture of $H_2$ and $D_2$. These findings unambiguously show that the 4145, 2985, and 3626 cm$^{-1}$ lines are vibrational modes of $H_2$, $D_2$, and HD, respectively.

Thermal treatment of ZnO at 1000 °C results in a preferential loss of oxygen atoms and, subsequently, to the formation of oxygen vacancies $V_O$ [34,35]. The concentration profile of $V_O$ is strongly nonuniform with the maximum value to be found at the sample surface [29]. An oxygen vacancy readily traps $H_{BC}$ and forms a shallow donor $H_O$ with an ionization energy of 47 meV [29]. In Raman spectra, $H_O$ is detected via internal $1s \rightarrow 2s(p)$ donor transition at 265 cm$^{-1}$ [36]. We found that the concentration profiles of $H_O$ and $H_2$ anticorrelate. This implies that relative strengths of the Raman signals due to $H_2$, HD, and $D_2$ depend on the sample depth, and the intensities given in the top spectrum of Fig. 2 cannot be directly related to the H-to-D isotope ratio during the treatment.

We also note that the weak intensity of the $H_2$ line compared to that of $H_{BC}$ shown in Fig. 1 does not imply that only a small fraction of $H_{BC}$ forms molecular hydrogen. Intensities of Raman lines depend on many parameters such as type of chemical bond, host semiconductor, excitation laser frequency, charge state of the defect, etc. A separate investigation will be performed to calibrate the concentration of $H_2$ from the Raman data.

First-principles calculations predict a stretch mode of $H_2$, $D_2$, and HD trapped at the interstitial site of the ZnO lattice at frequencies of 4032, 2852, and 3497 cm$^{-1}$, respectively [37]. The computational method employed in Ref. [37], however, seems to underestimate the experimental values by about 100 cm$^{-1}$. Taking into account this systematic correction we assign the 4145 cm$^{-1}$ mode to interstitial $H_2$ in ZnO.

The hydrogen molecule consists of two equivalent nuclei with spin 1/2. Thus, the total nuclear spin of $H_2$ is either 0 or 1. These states are referred to as para- and ortho-$H_2$, respectively. The protons are fermions, and according to the Pauli principle the total wave function of the molecule must be odd with respect to permutations of the nuclei. Since the spin wave function of para-$H_2$ is odd, the rotational wave function must be even with even values of $J$, the rotational quantum number. The $J$ values of ortho-$H_2$ must be odd [38].

Because of rovibrational coupling, the frequency of the stretch mode of $H_2$ depends on the rotational state $J$. This leads to different frequencies of the stretch modes of ortho- and para-$H_2$. The difference in frequencies between the

modes with $J = 1$ and $J = 0$, which are referred to as the $Q_1(1)$ and $Q_1(0)$ states, respectively, is called the ortho-para splitting. For free $H_2$ it equals 6 $cm^{-1}$ [33], whereas for interstitial $H_2$ trapped in semiconductors the ortho-para splitting was found to be around 8–9 $cm^{-1}$ [3,6,8].

A large magnetic field gradient is needed to transfer ortho- to para-$H_2$ [39]. Under ''normal'' conditions (low pressure gaseous phase, nonparamagnetic host, no magnetic impurity nearby) the two states do not thermalize and once formed, ortho- and para-$H_2$ remain independent. In Si, for example, it takes more than 500 h at 77 K to reach thermal equilibrium for interstitial ortho- and para-$H_2$ [7].

Since our ZnO samples were kept at room temperature, one should expect that both ortho- and para-$H_2$ will appear in the ratio determined solely by the degeneracy of the nuclear spin states, $(2 \times 1 + 1):(2 \times 0 + 1) = 3:1$. Figure 3 shows a Raman spectrum of $H_2$ in ZnO taken with a resolution of 2.5 $cm^{-1}$. In addition to the 4145 $cm^{-1}$ line, a weaker component blueshifted by 8 $cm^{-1}$ is also present in the spectrum. The two lines appear in the spectrum with intensities close to the expected ortho-to-para ratio 3:1. This result is fully consistent with the model of $H_2$ as a free rotator located at the interstitial site of the ZnO lattice. Table I summarizes the experimental and theoretical frequencies of the vibrational modes due to the $H_2$ molecule in ZnO. For comparison, we also give the stretch modes of $H_2$ in vacuum [33].

The formation of the $H_2$ molecule depicted in Fig. 1 has to be considered in more detail. According to first-principles calculations, $H_{BC}$ is the ground state of hydrogen in ZnO for nearly all Fermi level energies except those close to the conduction band minimum [28]. This is consistent with our results: Directly after the high temperature hydrogenation most hydrogen occupies the bond-centered site of the ZnO lattice and gives rise to the 3611 $cm^{-1}$ stretch mode [29]. Bond-centered hydrogen is a shallow donor with an ionization energy of 53 meV [29], and the $H_{BC}$ concentration determines the Fermi level position in our nominally undoped ZnO samples. As the Fermi level approaches the bottom of the conduction band, $H_2$ becomes energetically more favorable compared to $H_{BC}$ [28]. Therefore, $H_{BC}$ occurring in high concentrations should not be stable against the formation of $H_2$. With the parameters employed in this study, the amount of $H_{BC}$ in our samples directly after the treatment was around $10^{18}$ $cm^{-1}$ [13,29]. This quantity ensures that the Fermi level is positioned at the bottom of the conduction band, which, in turn, implies that isolated hydrogen should eventually convert into $H_2$. This formation process of $H_2$ in ZnO is consistent with theory.

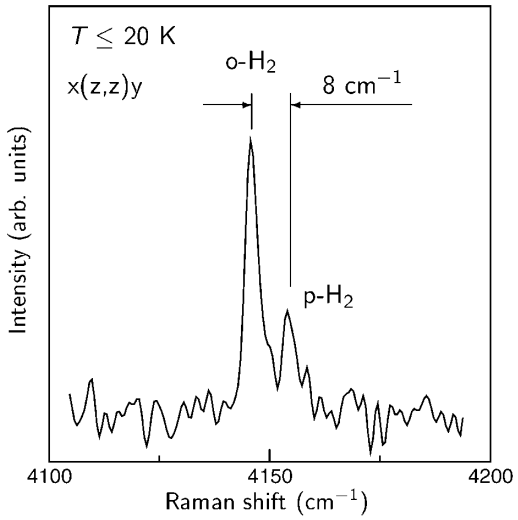


FIG. 3. Raman spectrum of a ZnO sample measured at $T \leq 20$ K in the $x(z, z)y$ geometry. The sample was treated at 1000 °C for 1 h in $H_2$ gas and subsequently annealed at 500 °C. Spectral resolution is 2.5 $cm^{-1}$.

Finally, we comment on the diffusion of hydrogen in ZnO. Theory predicts an activation energy of $H_{BC}$ in ZnO below 0.5 eV [40]. This means that isolated hydrogen should be very mobile already at room temperature. Secondary ion mass spectrometry data on ZnO samples exposed to a deuterium plasma seem to be consistent with theory: The activation energy for deuterium diffusion was found to be $0.17 \pm 0.12$ eV [41].

The elementary diffusion step of hydrogen in ZnO was recently studied by stress-induced dichroism of the CuH complex. The results were linked to hydrogen diffusion, and it was suggested that the activation energy of hydrogen motion in ZnO is around 0.5 eV [42]. These results disagree with the early studies of hydrogen diffusion in ZnO. Mollwo [12] and Thomas and Lander [13] investigated hydrogen diffusion by detecting the change in conductivity of the ZnO samples. They suggested that hydrogen diffusion in ZnO occurs with an activation energy of 0.9–1.1 eV.

Our results on $H_2$ imply, however, that the experiments by Mollwo and Thomas and Lander should be reconsidered. The hydrogen molecule is electrically inactive and, therefore, cannot be directly detected in conductivity measurements. Moreover, the Coulomb repulsion between the two neighboring, positively charged $H_{BC}$ defects should contribute to the stability and/or diffusion of hydrogen in ZnO and thus result in an enhancement of the apparent activation energy of hydrogen diffusion determined from conductivity experiments.

TABLE I. Experimental and theoretical frequencies of $H_2$ in ZnO ($cm^{-1}$). The values for free $H_2$ are given for comparison.

| Isotope | Mode | Free $H_2$ [33] | Exp. | Theory [37] |
|---|---|---|---|---|
| $H_2$ | $Q_1(0)$ | 4161 | 4153 | 4032 |
| | $Q_1(1)$ | 4155 | 4145 | |
| HD | $Q_1(0)$ | 3632 | 3626 | 3497 |
| $D_2$ | $Q_1(0)$ | 2994 | 2985 | 2582 |
| | $Q_1(1)$ | 2991 | | |

In conclusion, the results of Raman scattering studies on vapor phase grown ZnO hydrogenated via annealing in hydrogen and/or deuterium atmospheres are presented. It is determined that the hidden hydrogen in ZnO occurs in the form of interstitial $H_2$. The molecule is a free rotator with the stretch modes of para- and ortho-$H_2$ being 4153 and 4145 $cm^{-1}$, respectively.

The authors are indebted to R. Helbig for providing us with the ZnO samples. M. Stavola is greatly acknowledged for numerous and helpful discussion. S. Koch is acknowledged the help with the samples preparation.

*edward.lavrov@physik.tu-dresden.de

[1] A. Mainwood and A. M. Stoneham, Physica (Amsterdam) **116B+C**, 101 (1983).
[2] J. W. Corbett, S. N. Sahu, T. S. Shi, and L. C. Snyder, Phys. Lett. **93A**, 303 (1983).
[3] J. Vetterhöffer, J. Wagner, and J. Weber, Phys. Rev. Lett. **77**, 5409 (1996).
[4] V. P. Markevich and M. Suezawa, J. Appl. Phys. **83**, 2988 (1998).
[5] G. A. Shi, M. Stavola, W. B. Fowler, and E. E. Chen, Phys. Rev. B **72**, 085207 (2005).
[6] M. Hiller, E. V. Lavrov, and J. Weber, Phys. Rev. B **74**, 235214 (2006).
[7] M. Hiller, E. V. Lavrov, and J. Weber, Phys. Rev. Lett. **98**, 055504 (2007).
[8] M. Hiller, E. V. Lavrov, J. Weber, B. Hourahine, R. Jones, and P. R. Briddon, Phys. Rev. B **72**, 153201 (2005).
[9] G. A. Shi, M. Saboktakin, M. Stavola, and S. J. Pearton, Appl. Phys. Lett. **85**, 5601 (2004).
[10] Ü. Özgür, Ya. I. Alivov, C. Liu, A. Teke, M. A. Reshchikov, S. Doğan, V. Avrutin, S.-J. Cho, and H. Morkoç, J. Appl. Phys. **98**, 041301 (2005).
[11] C. Klingshirn, Phys. Status Solidi B **244**, 3027 (2007).
[12] E. Mollwo, Z. Phys.. **138**, 478 (1954).
[13] D. G. Thomas and J. J. Lander, J. Chem. Phys. **25**, 1136 (1956).
[14] F. G. Gärtner and E. Mollwo, Phys. Status Solidi B **89**, 381 (1978).
[15] S. F. J. Cox *et al.*, Phys. Rev. Lett. **86**, 2601 (2001).
[16] K. Shimomura, K. Nishiyama, and R. Kadono, Phys. Rev. Lett. **89**, 255505 (2002).
[17] D. M. Hofmann, A. Hofstaetter, F. Leiter, H. Zhou, F. Henecker, B. K. Meyer, S. B. Orlinskii, J. Schmidt, and P. G. Baranov, Phys. Rev. Lett. **88**, 045504 (2002).
[18] E. V. Lavrov, J. Weber, F. Börrnert, C. G. Van de Walle, and R. Helbig, Phys. Rev. B **66**, 165205 (2002).
[19] M. D. McCluskey, S. J. Jokela, K. K. Zhuravlev, P. J. Simpson, and K. G. Lynn, Appl. Phys. Lett. **81**, 3807 (2002).
[20] C. H. Seager and S. M. Myers, J. Appl. Phys. **94**, 2888 (2003).
[21] B. K. Meyer, H. Alves, D. M. Hofmann, W. Kriegseis, D. Forster, F. Bertram, J. Christen, A. Hoffmann, M. Straßburg, M. Dworzak, U. Haboeck, and A. V. Rodina, Phys. Status Solidi B **241**, 231 (2004).
[22] L. E. Halliburton, L. Wang, L. Bai, N. Y. Garces, N. C. Giles, M. J. Callahan, and B. Wang, J. Appl. Phys. **96**, 7168 (2004).
[23] E. V. Lavrov, F. Börrnert, and J. Weber, Phys. Rev. B **72**, 085212 (2005).
[24] E. V. Lavrov and J. Weber, Phys. Status Solidi B **243**, 2657 (2006).
[25] G. A. Shi, M. Stavola, and W. B. Fowler, Phys. Rev. B **73**, 081201(R) (2006).
[26] S. J. Jokela and M. D. McCluskey, Phys. Rev. B **76**, 193201 (2007).
[27] E. V. Lavrov, J. Weber, and F. Börrnert, Phys. Rev. B **77**, 155209 (2008).
[28] C. G. Van de Walle, Phys. Rev. Lett. **85**, 1012 (2000).
[29] E. V. Lavrov, F. Herklotz, and J. Weber, Phys. Rev. B **79**, 165210 (2009).
[30] G. Müller and R. Helbig, J. Phys. Chem. Solids **32**, 1971 (1971).
[31] R. Helbig, J. Cryst. Growth **15**, 25 (1972).
[32] G. A. Shi, M. Stavola, S. J. Pearton, M. Thieme, E. V. Lavrov, and J. Weber, Phys. Rev. B **72**, 195211 (2005).
[33] B. P. Stoicheff, Can. J. Phys. **35**, 730 (1957).
[34] H. E. Brown, *Zinc Oxide: Properties and Applications* (International Lead Zinc Research Organization, New York, 1976).
[35] A. F. Kohan, G. Ceder, D. Morgan, and C. G. Van de Walle, Phys. Rev. B **61**, 15019 (2000).
[36] E. V. Lavrov, F. Herklotz, and J. Weber (to be published).
[37] M. G. Wardle, J. P. Goss, and P. R. Briddon, Phys. Rev. B **72**, 155108 (2005).
[38] L. D. Landau and E. M. Lifshits, *Quantum Mechanics: Nonrelativistic Theory* (Pergamon, London, 1959).
[39] E. Wigner, Z. Phys. Chem., Abt. B **23**, 28 (1933).
[40] M. G. Wardle, J. P. Goss, and P. R. Briddon, Phys. Rev. Lett. **96**, 205504 (2006).
[41] K. Ip, M. E. Overberg, Y. W. Heo, D. P. Norton, S. J. Pearton, C. E. Stutz, B. Luo, F. Ren, D. C. Look, and J. M. Zavada, Appl. Phys. Lett. **82**, 385 (2003).
[42] F. Börrnert, E. V. Lavrov, and J. Weber, Phys. Rev. B **75**, 205202 (2007).